Silicomanganese alloy from rich manganese slag produced from Egyptian low-grade manganese ore

by H. El-Faramawy[1], M. Eissa[1], S.N. Ghali[1], T. Mattar[1], A. Ahmed[1], M. El-Fawakhry[1], and E.M. Kotb[1]

Affiliation:
[1]Central Metallurgical Research and Development Institute (CMRDI), Cairo, Egypt.

Correspondence to:
S.N. Ghali

Email:
a3708052@gmail.com

Dates:
Received: 2 Jun. 2021
Revised: 23 Sep. 2021
Accepted: 29 Nov. 2021
Published: January 2022

How to cite:
El-Faramawy, H., Eissa, M., Ghali, S.N., Mattar, T., Ahmed, A., El-Fawakhry, M., and Kotb, E.M. 2022
Silicomanganese alloy from rich manganese slag produced from Egyptian low-grade manganese ore.
Journal of the Southern African Institute of Mining and Metallurgy, vol. 122, no. 1, pp. 5-14

DOI ID:
http://dx.doi.org/10.17159/2411-9717/1648/2022

ORCID:
H. El-Faramawy
https://orcid.org/0000-0002-1828-0501
M. Eissa
https://orcid.org/ 0000-0001-8688-0843
S.N. Ghali
https://orcid.org/ 0000-0002-9195-0663
T. Mattar
https://orcid.org/ 0000-0002-5659-208X
A. Ahmed
https://orcid.org/ 0000-0002-2264-4195
M. El-Fawakhry
https://orcid.org/ 0000-0002-1258-8492
E.M. Kotb
https://orcid.org/0000-0002-7488-6006

Synopsis

As a result of the depletion of high-grade manganese reserves, it has become necessary to consider the exploitation of low-grade manganese ores. The main problem of low-grade manganese ore is the low Mn/Fe ratio, which makes it unfit for the production of manganese ferroalloys. In this work, a selective reduction technique was used for smelting low-manganese ore in the presence of coke and fluxing material in an electric submerged arc furnace to obtain a rich manganese slag and low-manganese pig iron. The product slag was blended with medium-manganese ore and smelted in an electric submerged arc furnace, in the presence of coke and the fluxing agent, to produce silicomanganese alloy. The influence of reducing agent ratio, charge basicity, and charge Mn/Si ratio on the smelting process was investigated. The optimum conditions were found to be a coke ratio of, 1.35, Mn/Si ratio of 2.0, and charge basicity of 2.5. The silicomanganese alloy produced under these conditions satisfies the specifications for Si16Mn63 and Si17Mn65. The experimental results were applied on a pilot scale, producing a silicomanganese alloy with a chemical composition close to that of the standard specifications.

Keywords

silicomanganese, low-grade manganese ore, medium-manganese ore, carbothermic reduction, submerged arc furnace.

Introduction

Silicomanganese alloy is used as a source of silicon and manganese in steelmaking to produce different steel grades. It is also used as a deoxidizer in place of both ferrosilicon and ferromanganese. The consumption of silicomanganese is increasing as a result of growing steel production. Steelmakers prefer to utilize silicomanganese instead of both FeSi and FeMn due to several advantages, such as its low cost and greater effectiveness as a deoxidizer. Also, when used with aluminium to produce an effective complex manganese-silicon-aluminium deoxidizer, it causes less contamination from phosphorus, carbon, aluminium, and nitrogen in steel compared with the FeSi and FeMn mixture (Ahmed *et al.*, 2014).

The Om Bogma manganese deposit in Egypt contains reserves of about 1.7 Mt, most of which are low-grade ores. Many studies have been carried out using ore dressing to separate the manganese oxides from the ore. The separation of manganese impurities by magnetizing roasting followed by low-intensity magnetic separation is not possible, owing to the mineralogical complexity of the ore. Unfortunately, ore dressing studies have proved that the elimination of manganese oxides present in iron ore is not successful.

In recent years, a programme of work has been initiated in the Steel and Ferroalloys Department, Central Metallurgical Research and Development Institute (CMRDI), aimed at the selective reduction of low-grade manganese ore in an electric submerged arc furnace to separate pig iron and produce a high-manganese slag for the production of manganese ferroalloys. The use of such slag in the production of silicomanganese alloys is very attractive from an economic point of view. High-manganese slag is characterized by a high manganese content, low excess oxygen, high Mn/Fe ratio, low fines content, low phosphorus content, and low cost (Eissa *et al.*, 2004). Mn-rich slags produced from the injection of high-manganese pig iron were found to have levels of Mn >35%, (Mn)/(Fe) >7.65, (Mn)/(P) >285, and with both Mn- and Fe-oxides existing as lower oxides (MnO and FeO) (El-Faramawy *et al.*, 2004).

Generally, silicomanganese is produced in an electric arc furnace by carbothermic reduction of manganese ores, high-manganese slag, and quartz in the presence of fluxing materials. The process in which high-carbon ferromanganese is produced using acidic rich-slag practice with subsequent

silicomanganese production from the high-Mn slag is sometimes referred to as the duplex process. This process is different from the other practice, in which only Mn ore is utilized as source of manganese and the product slag is discarded (Steenkamp and Basson, 2013).

The most important reactions taking place during the process, the reduction of MnO and SiO_2, are shown in Equations [1]–[3] (Jana, and Randhawa, 2009; Olsen, Tangstad, and Lindstad, 2007). The components such as MnO and SiO_2 can be reduced simultaneously during the smelting process.

$$SiO_{2(l)} + 2C_{(s)} \rightarrow Si_{(l)} + 2CO_{(g)} \quad [1]$$

$$MnO_{(l)} + C_{(s)} \rightarrow Mn_{(l)} + CO_{(g)} \quad [2]$$

$$2MnO_{(l)} + Si_{(l)} \rightarrow SiO_{2(l)} + 2Mn_{(l)} \quad [3]$$

Equations [1] and [2] are independent reactions and can be combined to form Equation [4].

$$MnO + SiO_2 + 3C \rightarrow MnSi + 3CO \quad [4]$$

At the process temperature of 1600°C, reduction of MnO to metallic manganese by solid carbon occurs according to Equation [2]. However, the reduction of SiO_2 to metallic silicon by solid carbon (Equation [1]) cannot occur due to the high free energy requirement at that temperature (Olsen, 2016). The reduction of SiO_2 to silicon metal by solid carbon at 1600°C can only take place in the presence of metallic Fe and Mn, which lower the activity of silicon in the alloy (Davidsen, 2011). According to Equation [3], SiO_2 reduction occurs when the activity of SiO_2 in the slag is suffiiciently high due to the decrease of MnO activity caused by the complete reduction of MnO (Kor, 1979). The other components, such as CaO, Al_2O_3, and MgO, remain stable during the smelting process and inflluence the activity of both SiO_2 and MnO in the slag.

The formation of silicon carbide has to be considered in the silicomanganese process. The carbon concentration in the silicomanganese alloy is affected mainly by the silicon content. With increasing silicon content in the alloy, carbon becomes less stable and carbides become the dominant stable phase, which leads to a decrease in the concentration of dissolved carbon in the alloy (Alex *et al*., 2007). The percentage of carbides increases with increasing total carbon in the alloy. In addition, temperature also has an important effect on the carbon concentration in two ways. A higher temperature increases the carbon solubility at constant silicon content, and also increases the silicon content, which therefore decreases the carbon concentration (Anacleto, Ostrovski, and Ganguly, 2006). Thermodynamically, when the silica activity in the slag exceeds 0.2 at 1600°C, silicon carbides start to form according to Equation [5] (Olsen, and Tangstad, 2004);

$$Si + C \rightarrow SiC \quad [5]$$

Silicomanganese slag basicity (B) is expressed as the ratio between the basic and acid slag constituents, as illustrated in Equation [6]. According to equilibrium studies by earlier researchers, an alternative measurement of slag basicity, the R-ratio (Equation [7]) was used due to its strong inflluence on SiO_2 activity in the slag and, therefore, its signifiicant effect on the alloy composition (Tang, and Olsen, 2004; Ding and Olsen 2000)

$$B = \frac{CaO + MgO}{SiO_2} \quad [6]$$

$$R = \frac{CaO + MgO}{Al_2O_3} \quad [7]$$

where all constituents are expressed in terms of weight per cent. Hence the composition and thermodynamic properties of slag are vital in determining the alloy composition, as they affect the distribution of Mn and Si across the slag-metal interface and thus the recovery of the metals in the desired ratio (Olsen, 2016; Tranell *et al*., 2007).

Nikolaev (1974) reported the optimum R-value to be 2.5, whereas Emlin *et al*., (1986) found the optimum R-value to be in the range of 1.2–2.2. These researchers also found that the basicity of slag was best adjusted through the addition of dolomite, which gives higher silicon- and manganese recoveries compared with the addition of limestone only or with dolomite. Other equilibrium studies (Ding and Olsen 2000; Olsen and Tangstad, 2004; Tang and Tangstad, 2007) concluded that the R-ratio strongly influences the SiO_2 activity of the slag and thereby the Si content of the alloy.

As the basic oxides content is increased by the addition of dolomite, the interaction between Ca^{2+}, Mg^{2+}, and silicate ions becomes stronger than that between Mn^{2+} and silicate ions, resulting in the formation of stable Ca and Mg silicates (Kubaschewsky, Evans, and Alcock, 1979; Barin, 1989). This gives rise to free Mn^{2+} ions, which kinetically associate, with free O^{2-} ions in the slag and increase aMnO in the slag. The high MnO in the slag favours the transfer of Mn into the metal. In contrast, $a$$SiO_2$ in the slag is diminished by the addition of basic oxides, which adversely affects the Si content of the alloy. Therefore, it is clear that maintaining the appropriate concentrations of both basic oxides and silica is required in order to yield the desired grade of SiMn alloy (Barin, 1989).

Silicomanganese smelting is carried out in an acidic slag with basicity lower than unity ($B < 1$) and defined as B = (CaO, wt%. + MgO, wt%)/(SiO_2, wt%). Several studies have been done on the effect of slag basicity on Mn and Si distribution. The distribution ratio of an element is defined as the percentage of that element in the slag phase divided by the percentage in the metal phase. Equilibrium studies on the distribution of Mn between Mn-Si-Fe-C alloys and MnO-CaO-MgO-SiO_2-Al_2O_3 slag at 1500°C under CO atmosphere revealed that an increase in the basicity ratio of the slag decreases the Mn distribution ratio (Cengizler, 2003). In contrast, by increasing the silica concentration of the slag the Mn distribution ratio increases. The addition of alumina to the slag favours the transfer of Mn to the alloy, leading to a low MnO content in the slag. Cengizler, Eric, and Reuter (1997) modelled activity data for ferromanganese slags by applying neural nets at 1500°C for slag compositions in the range MnO 5–40%, CaO 4–35%, MgO 0.3–38%, SiO_2 25–60%, and Al_2O_3 2.5–7%. They found that the MnO activity coefficient in liquid slag varies on both sides of unity. Tang, and Olsen (2006) and Ding and Olsen (2000) concluded that the addition of alumina to acidic slag decreases the equilibrium MnO content in the slag. They also found that the activity coefficient (Ý) of MnO is less than unity in acidic slags, whereas ÝMnO > 1 in basic slags.

Viscosity is one of the most important properties of the slag and a critical parameter for many smelting processes. The viscosity of slag depends on slag composition, oxygen partial

pressure, and temperature. Viscosity, being the viscous resistance of the melt in the flow process, predominantly relies on the large, complex silica anions (*e.g.*, SiO_4^{4-}, $Si_2O_7^{6-}$, and $Si_7O_{10}^{8-}$). Hence, a high SiO_2 content will increase the viscosity. Silica forms complex network crystals containing Si-O bonds, resulting in low recoveries of valuable metal from the slag. The network structure is destroyed if an appropriate amount of basic oxides is added to the molten slag (Olsen, Tangstad, and Lindstad, 2007), which promotes the further recovery of metals from the slag. In absence of a flux (*i.e.* dolomite) the Mn ore, and recycled slag are the sources of the CaO, MgO, and Al_2O_3, which form slag upon melting.

The difficulty and high cost of measuring slags viscosity have led to the development of numerous viscosity models. Viscosities and densities of typical HCFeMn and SiMn slags were calculated at a standard operating temperature of 1673 K for HCFeMn slags and 1873 K for SiMn slags. The calculations considered the percentage solids derived from the equilibrium phase composition determined with FactSage (Muller, Zietsman, and Pistorius, 2015). In this work, Weymann-Frenkel's equation was used for determining the slag viscosity as a function in temperature and chemical composition (Ray and Pal, 2004) as given in Equation [8].

$$\eta = A * T * exp\frac{1000 * B}{T} \quad [8]$$

where η is viscosity, *T* is temperature, and A and B are independent parameters calculated according to the Urbain model (Rosypalová *et al.*, 2014)

This investigation aims at studying the possibility of using high-manganese slag obtained from Egyptian low-grade manganese ore in the production of standard silicomanganese alloy. Different parameters affecting the production process were studied using a bench-scale submerged arc furnace, and the obtained optimum conditions were implemented on the pilot plant scale.

Experimental

About 1 t of manganese-rich slag was produced on the pilot scale in the Steel and Ferroalloys Technology Department at the Central Metallurgical Research and Development Institute by selective reduction of low-grade manganese ore and used in the production of silicomanganese alloy.

Manganese ore, quartzite, dolomite, bauxite, and coke nut were suppled from Sinai Manganese Company. The raw materials were crushed in a jaw crusher to –55 mm (manganese-rich slag and medium-grade manganese ore), –35 mm (quartzite, dolomite), –10 mm (bauxite), and –25 mm (coke nut). All the raw materials were analysed by X-ray fluorescence. The chemical compositions of the raw materials are listed in Table I. Manganese minerals are complex and orebodies are also typically comples, hence the manganese ore composition is expressed in terms of Mn only, except where mineralogical information is available that will determine the manganese distribution between Mn/Mn^{2+}, Mn^{3+}, and Mn^{4+} (Steenkamp *et al.*, 2020). The Mn-rich slag and medium-grade Mn ore ware also subjected to XRD.

Nineteen experimental heats were carried out – sixteen on the bench scale and three on the pilot plant scale – to investigate the influence of reducing agent ratio, charge basicity, and charge Mn/Si ratio on metal yield and recoveries of Mn and Si. The bench-scale SAF (Figure 1) is an open furnace operated with a reducing atmosphere. The power is supplied to the furnace through an AC stepwise transformer with primary electric power of 380 V and 220 A. The furnace transformer operates at a maximum current of 2000 A at different voltages ranging from 0 to 70 V passed through two 40 mm graphite electrodes that can be raised and lowered manually. The furnace shell is 340 mm in diameter and

Table I

Chemical composition of the raw materials (wt%)

Constituents	Mn-rich slag	Medium-grade Mn ore	Quartzite	Dolomite	Bauxite	Coke	Coke ash
MnO_2	50.56	43.7					0.68
MnO		20.05					
$Mn_{tot.}$	39.17	42.9	0.286	0.73	0.90		15.26
Fe_2O_3	5.36	19.0					
FeO							
$Fe_{tot.}$	4.17	13.3	98.338	9.43	1.50		46.18
SiO_2	13.18	6.12					
CaO	5.12	3.62	0.430	27.00	0.10		2.97
MgO	5.587	1.15	0.0450	16.65	0.05		0.27
Al_2O_3	3.40	4.00	0.212	0.44	85.00		32.87
P	0.067	0.45					0.030
K_2O	2. 89	0.297		0.01	0.02		
Na_2O	2.965	0.243		0.02	0.10		
BaO	4.02	1.25					
V_2O_5	1.80	0.011					
TiO_2	3.50	0. 022	0.22	2.24	1.50	0.20	0.98
S	0.52	0.001					0.132
ZrO_2	0.25		0.21	42.56	10.00		0.030
LOI							
Fixed carbon						85.47	
Ash content						12.90	
V.M						0.58	
Moisture			0.11			0.80	
Hum.				0.34			
Total	99.219	99.914	99.851	99.42	99.17	99.95	99.40
Mn/Fe	9.39	3.23					

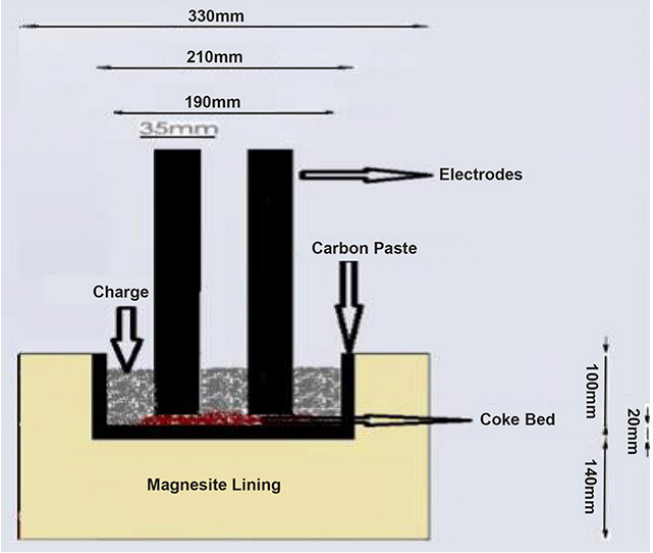

Figure 1—Schematic diagram of the bench-scale SAF

300 mm in height. The shell wall and bottom were lined with a thick rammed magnesite layer, using dead-burned magnesia with the chemical composition MgO 88%, CaO 7%, SiO_2 1%, Al_2O_3 1%, Fe_2O_3 3%, and grain size 0-5 mm, supplied by Delta Steel Mill Company. The thickness of the magnesite layer was 60 mm for the wall and 100 mm for the bottom. The magnesite layer was lined with an inner lining of carbon paste, supplied by Sinai Manganese Company as unbaked paste with the composition fixed C 82%, volatiles 13%, ash 4.6%, P 0.02%, and S 0.38%. The furnace was operated at 45 V and 550 A, and the smelting temperature ranged from 1600 to 1650°C, measured optically using an infra-red pyrometer. The accuracy of the pyrometer readings was validated by limited measurements using an immersion thermocouple.

The 100 kVA pilot-scale SAF is an open furnace with a water-cooled roof. The furnace transformer supplies a maximum current of 2080 A at voltages ranging from 35 to 100 V passed through two 75 mm diameter non-tilting graphite electrodes that can be raised or lowered manually. The pilot SAF was operated at the same operating power and temperature conditions as used in the bench-scale work, and was lined with the same materials. The product alloy and slag were cast in metal moulds, and representative samples were taken for chemical analysis using a portable XRF instrument. The chemical analyses were validated using XRF.

Using FactSage-based design calculations for the production of high-carbon ferromanganese on a pilot scale, Steenkamp (2020) found the recoveries of Mn and Fe at equilibrium conditions to be 76–97% and 100%, respectively. A comparison of Mn ferroalloy smelting in pilot-scale AC and DC submerged arc furnaces showed the Mn recovery to alloy to be 82.1 + 0.5% (AC) and 83.4 + 0.5% (DC) for FeMn smelting, and 69–70% and 70–80% for SiMn (Lagendijk *et al*., 2010).

By adjusting the slag composition and fluxing materials in the pilot-scale smelting of SiMn by using a Mn-rich slag in the charge, SiMn alloy containing 73% Mn, 15% Si, and 1.1% C has been produced with a metal yield of 65% and 70% Mn recovery (Eissa *et al*., 2004).

The Mn/Fe ratio for the most popular grades of SiMn alloys – Si16Mn63, Si19Mn63, and Si18Mn68 – ranges between 3.5 and 6. (Bureau of Indian Standards. 2013). Due to the lower Mn recovery compared to Fe recovery in the SiMn smelting process, the Mn/Fe ratio of the charge should be higher than the target Mn/Fe ratio of the product alloy The Mn/Fe ratio of manganese-rich slag produced from low-grade manganese ore is about 9.39, as shown in Table I. This ratio is suitable to compensate for the low Mn/Fe ratio of the medium-grade manganese ore. The blend of manganese-rich slag and medium-grade manganese ore contains a relatively high Mn/Fe ratio and is suitable to be used for production of silicomanganese alloy.

At first, the quantities of coke required for the reduction of different blends, and the quantities of fllux material to attain different ratios of $(CaO+MgO)/(Al_2O_3)$ were calculated. Manganese ores and slag with the designed Mn/Fe ratios and the required quartzite were identified.

Manganese-rich slag was mixed with medium-grade manganese ore, quartzite, coke, and dolomite. The furnace was preheated, and the graphite electrodes were lowered to a position near the bottom lining of the furnace. A layer of coke bed was charged between the electrode tips. Then the current was switched on to strike an electric arc, which raises the furnace hearth temperature, and the mixed charge was divided into three parts and charged gradually. The furnace was operated at 45 V and a current of around 550 A from the start of charging until casting. After the complete smelting of the blend, the molten metal and slag were left inside the furnace for enough time to ensure the complete reduction and settling of the silicomanganese alloy. The product silicomanganese alloy and discard slag were then cast into metal moulds of 100 mm inner diameter and 150mm height where the metal, covered by the slag, was left to cool to room temperature.

Based on the optimum conditions of coke ratio, basicity, and charge Mn/Si ratio in the blend that resulted in the highest yield and recoveries of Mn and Si, further heats of the silicomanganese alloy were performed in the 100 kVA pilot-scale submerged arc furnace. The product alloy and slag were cast into metal moulds of 300 mm diameter and 500 mm height and left to cool to room temperature. Representative samples of the metal and slag were analysed.

Results

The Egyptian low-grade manganese ore with a high iron content was upgraded by smelting the ore in an open submerged arc furnace. This smelting was performed with lower power and a deficiency of carbon in order to reduce most of the higher iron oxides to metallic iron while reducing the higher manganese oxides to MnO, which partitions predominantly to the slag phase. The smelting operation has to be strictly controlled, especially as regards the fixed carbon requirements, otherwise the pig iron will contain an unacceptable level of manganese. It is important to note that practically all the phosphorus will end up in the pig iron, thus leaving a P-free slag for silicomanganese production.

Several experimental heats were carried out to establish the optimum conditions for selective reduction of the iron to produce pig iron with the lowest manganese content and slag with the highest manganese content, lowest iron content, and highest Mn/Fe ratio. At the optimum conditions of power, coke addition, and charge basicity, 93% iron recovery was obtained in the pig iron product with 96% metal yield, and 90% MnO recovery to the slag. Adjusting the optimum smelting conditions produced pig iron with a low Mn content of 2–2.5% and a high-Mn slag containing 54% MnO and 3.2% FeO with a Mn/Fe ratio of 15.

The input and output materials for the sixteen experimental heats that were carried out on the bench scale SAF are listed in Table II. These experiments were done to study the effect of different parameters on the SiMn production process.

Effect of coke ratio

In the first series of experiments, seven heats (1-7) were carried out to investigate the influence of the coke ratio, which is the ratio of added coke to the stoichiometric requirement to reduce silicon, iron, and manganese oxides. In this series of tests, the blends comprised 2.5 kg of manganese-rich slag, 1.25 kg of medium-grade manganese ore, and 1.25 kg of quartzite, equivalent to 50%, 25%, and 25% by weight of the charge respectively. The coke weight ranged from 0.775 kg to 1.27 kg, corresponding to coke ratios from 0.95 to 1.55. All these tests were performed at a Mn/Fe ratio of 5.6. The metal yield and recoveries of manganese and silicon were calculated according to Equations [9]–[11]. The metal yield represents the weight of the product alloy divided by the theoretical alloy weight resulting from the complete reduction of the manganese, silicon, and iron in the charge and assuming a carbon content of 2% in the alloy. The manganese (and silicon) recovery represents the amount of manganese (silicon) in the product alloy divided by the total amount in the charge blend.

$$\%\ \text{Metal yield} = \frac{\text{wt. of produced alloy}}{((\sum \%\text{Mn}, \%\text{S}, \text{i} + \& \%\text{Fe in material (i)} * \text{wt. of material (i)in the blend})/100) * 1.02} * 100 \quad [9]$$

$$\%\ \text{Mn rec.} = \frac{\%\text{Mn} * \text{wt. of produced alloy}}{\sum(\%\text{Mn in material (i)} * \text{wt. of material (i)in the blend})} * 100 \quad [10]$$

$$\%\ \text{Si rec.} = \frac{\%\text{Si} * \text{wt. of produced alloy}}{\sum(\%\text{Si in material (i)} * \text{wt. of material (i)in the blend})} * 100 \quad [11]$$

The effects of the coke ratio on the metal yield and recoveries of manganese and silicon are illustrated in Figures 2 and 3 respectively. The chemical compositions of the silicomanganese alloys and slags produces are given in Table III.

Figures 2 and 3 indicate that the metal yield and recoveries of manganese and silicon increase with increasing coke ratio until a coke ratio of 1.35, then decrease slightly. Figure 3 shows that at a coke ratio of 1.0, manganese and silicon recoveries were low, and subsequently the manganese and silicon contents were below that in the standard silicomanganese alloy. With increasing coke ratio up to 1.35, both the manganese and silicon content in the product silicomanganese alloy increased as a result of the greater degree of reductions, leading to an increase in the metal yield.

The subsequent decline in the manganese and silicon recoveries with further increases in the coke ratio can be attributed to a few factors. Akil and Geveci (2008) stated that using carbon in excess of an optimum value may lead to the formation of an unreacted coke layer above the slag that probably hinders the settling of metal droplets from through the slag layer to the metal phase, thereby decreasing the quantity of alloy obtained. On the other hand, the coke ash contributes to slag formation. The ash content in coke is usually 8–13%. Approximately 75–80% of the coke ash is Al_2O_3+SiO_2, with an A/S ratio of about 0.65. The contribution of coke ash to the final slag is estimated to be around 5%. With increasing coke ratio, the

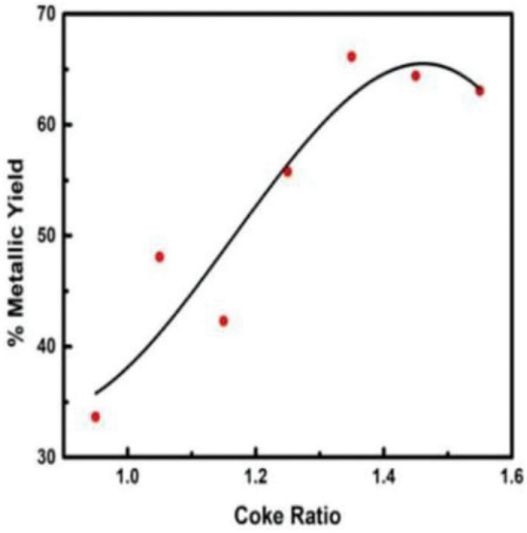

Figure 2—Effect of coke ratio on the metal yield of SiMn

Table II

Input and output materials for the experimental laboratory heats

Heat no.	Input charge (kg)						Operating conditions			Output	
	Mn-rich slag	Mn ore	Quartzite	Coke	Dolomite	Bauxite	Coke ratio	Charge basicity	Charge Mn/ Si ratio	Metal (kg)	Slag (kg)
1	2.5	1.25	1.25	0.775			0.95	1.95	1.99	0.875	1.6
2	2.5	1.25	1.25	0.86			1.05	1.95	1.99	1.25	1.3
3	2.5	1.25	1.25	0.94			1.15	1.95	1.99	1.1	0.4
4	2.5	1.25	1.25	1.02			1.25	1.95	1.99	1.45	1.15
5	2.5	1.25	1.25	1.1			1.35	1.95	1.99	1.72	0.3
6	2.5	1.25	1.25	1.19			1.45	1.95	1.99	1.675	1.1
7	2.5	1.25	1.25	1.27			1.55	1.95	1.99	1.64	1
8	2.5	1.25	1.25	1.1	0	0.1	1.35	1.3	1.99	1.3	0.45
9	2.5	1.25	1.25	1.1	0	0.06	1.35	1.5	1.99	1.45	2.6
10	2.5	1.25	1.25	1.1	0	0.03	1.35	1.7	1.99	1.5	1.5
11	2.5	1.25	1.25	1.1	0.135	0	1.35	2.3	1.99	1.72	1.2
12	2.5	1.25	1.25	1.1	0.215	0	1.35	2.5	1.99	1.8	0.95
13	2.5	1.25	1.25	1.1	0.295	0	1.35	2.7	1.99	1.62	1.22
14	2.85	1.4	0.75	1.07	0.215		1.35	2.5	3.07	1.7	0.9
15	2.65	1.35	1	1.09	0.215		1.35	2.5	2.45	1.77	1.9
16	2.35	1.15	1.5	1.12	0.215		1.35	2.5	1.63	1.77	0.85

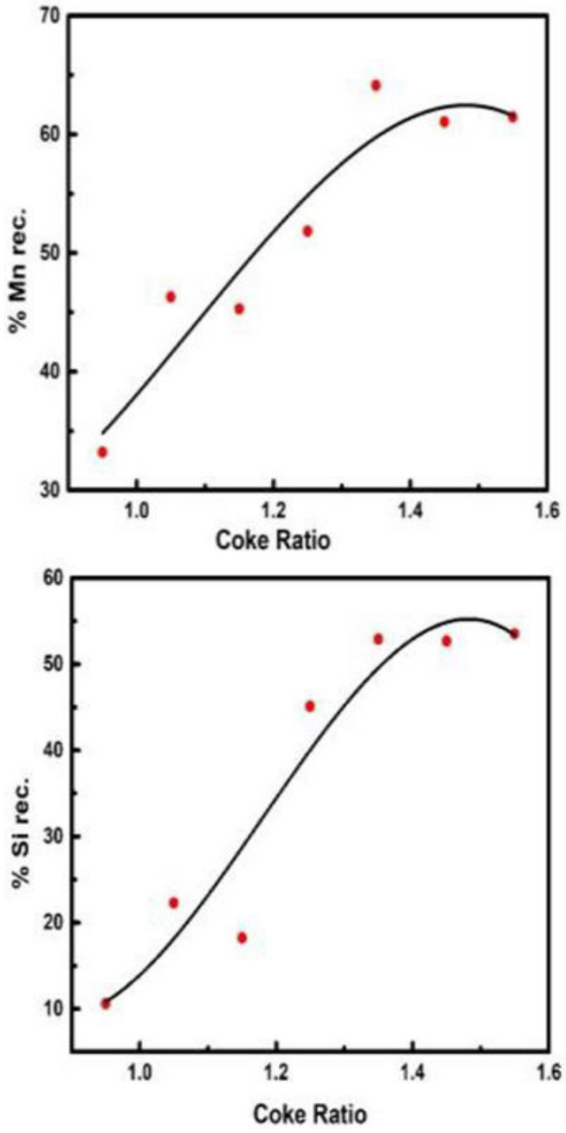

Figure 3—Effect of coke ratio on Mn and Si recoveries in SiMn

increase in coke ash leads to greater amounts of SiO_2 and Al_2O_3 in the slag and hence a higher viscosity which hinders the movement of metal droplets through the slag layer as indicated in Figure 4. Thus a lower metal yield and lower manganese and silicon recoveries were attained (Olsen, Tangstad, and Lindstad, 2007).

Effect of charge basicity

The second series of tests was designed to illustrate the influence of charge basicity on the smelting process. Seven heats (5, 8–13) were designed to investigate the influence of the charge basicity as (MgO + CaO) / Al_2O_3 on the metal yield and Mn and Si recoveries through the addition of either bauxite or dolomite. In this series, the blends were composed of 2.5 kg manganese-rich slag, 1.25 kg medium-grade manganese ore, and 1.25 kg quartzite, representing 50%, 25%, and 25% of the total charge weight respectively, with a coke ratio of 1.35. The charge basicity varied from 1.3 to 2.7, as given in Table II, and the Mn/Fe of all blends was 5.6.

The chemical composition of product alloy and slag is shown in Table III. The influence of charge basicity on metal yield is illustrated in Figure 5, while the effect on manganese and silicon recoveries is given in Figure 6. The graphs indicate that the metal yield and recoveries of both manganese and silicon increased as the charge basicity increased up to an optimum value of 2.5, beyond which the metal yield and recoveries decreased.

During silicomanganese production the silica content in the slag changes continuously due to the reduction of SiO_2. It is easier to control the basicity of the input materials than that of the produced slag. During smelting, both MnO and SiO_2 are reduced from the slag. So, the alternative measurement of slag basicity, (R) given by Equation [7], containing only nonreducible oxides, is more relevant than that given by Equation [6].

The requirements for greater reduction of manganese oxides are different to those for reduction of silicon oxides, *i.e.* a basic slag is required for manganese reduction and an acidic slag for silicon reduction. Hence, the composition of the charge and the operating conditions need to be balanced to obtain good recoveries and the desired grade of SiMn. An increase in the basicity of the slag, *i.e.*, increasing the proportion of basic oxides, leads to an increase in MnO activity and a decrease in SiO_2 activity in the slag. Therefore, more MnO and less SiO_2 is reduced by increasing the basicity of slag – in other words, increasing basicity decreases the equilibrium MnO and increases the equilibrium SiO_2 in the slag, as indicated in Figure 7 (Nokhrina, and Rozhikhina, 1998).

The influence of charge basicity on metal yield and manganese and silicon recoveries beyond the optimum can be discussed in terms of the effect of basicity on the viscosity of the slag. The

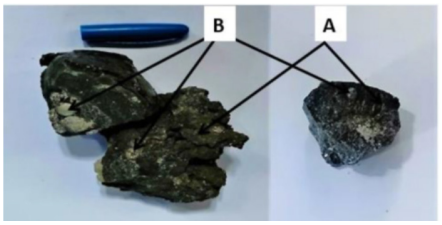

A, Discard slag and B, metal entrapment droplets

Figure 4—Photograph of metal droplets entrapped in discard SiMn slag

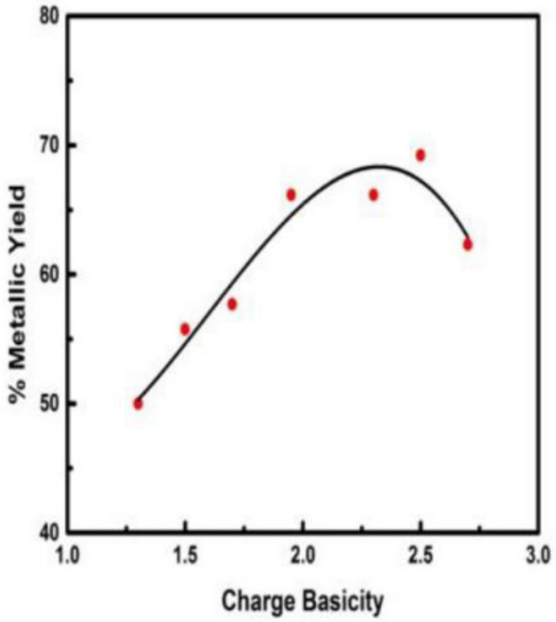

Figure 5—Effect of basicity on metal yield of SiMn

Table III

Chemical composition of the produced SiMn and discard slag from the bench-scale SAF

Heat no.	SiMn (wt%)					SiMn slag (wt%)						
	C	Mn	Si	S	P	MnO	SiO_2	Al_2O_3	CaO	MgO	BaO	S
1	2.399	57.5	9.26	0.018	0.057	32.31	45.64	5.9	6.36	5.87	1.7	0.412
2	2.07	56.1	13.6	0.016	0.069	27.14	45	7.18	8.37	6.94	2.75	0.392
3	2.08	62.4	12.65	0.013	0.06	22.91	44.09	9.42	9.65	8.48	2.8	0.4
4	1.72	54.17	23.73	0.02	0.04	15.9	42.56	11.8	10.95	12.4	3.91	0.332
5	0.91	56.5	23.46	0.0066	0.098	14	41.07	13.4	12.94	14.64	2.16	0.12
6	1.08	55.23	24	0.006	0.091	13.37	39.66	14.3	12.8	14.56	2.9	0.336
7	1.122	56.8	24.9	0.0058	0.1	13.46	39.14	14.11	13.23	15.1	2.46	0.42
8	1.22	52.16	19	0.006	0.112	15.81	45.43	13.5	10.55	9.65	2.7	0.52
9	2.02	61.8	17.83	0.004	0.072	13.71	42.07	14.2	11.9	13.1	3.22	0.16
10	1.79	59.1	20.89	0.005	0.07	14.22	43.29	12.12	10.79	13.73	3.61	0.212
11	0.8	60.5	21.7	0.0059	0.055	16.44	40.72	10.4	11.88	14.5	3.2	0.468
12	0.85	61.4	20	0.005	0.083	12.98	40.11	10.76	15.36	16.73	2.46	0.204
13	1.2	59.1	21.1	0.006	0.097	12.1	41.55	10.65	16.2	16.53	1.01	0.088
14	1.7	69	14	0.004	0.037	13.55	38.28	13.07	13.98	15.85	3.12	0.172
15	1.2	65.75	17.1	0.013	0.084	12.89	39.79	10.62	14.54	16.1	3.8	0.116
16	0.8	56.84	24.22	0.006	0.116	12.71	47.7	10.26	12.14	11.82	3.23	0.284

viscosities of the silicomanganese slag in this series of tests were calculated at 1600°C for different slag basicities using Equation [8] (Riss and Khodo, 1967; Rosypalová *et al.*, 2014) and plotted *versus* the final slag basicity. Figure 8 shows that the lowest viscosity, 6.3 poise, was attained for a slag basicity ratio CaO/SiO_2 of 0.37 and for (CaO + MgO)/Al_2O_3 at 2.5. The retardation of the reduction process at higher slag basicities beyond optimum conditions is the effect of the high viscosity of the slag, which seems to overcome the positive effect of increasing the MnO activity, with the net result of supressing the reduction process at

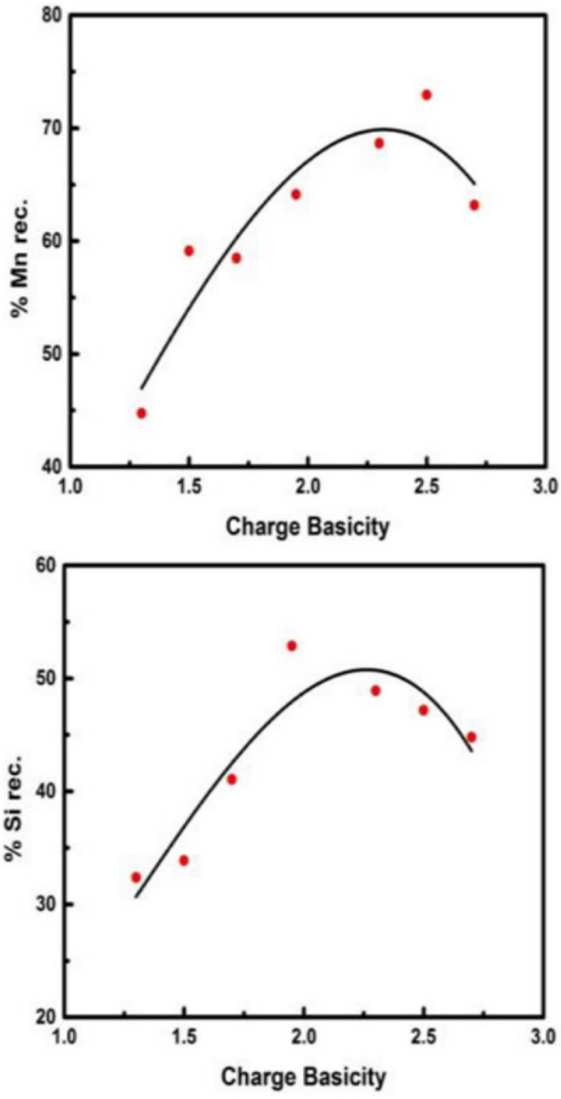

Figure 6—Effect of basicity on Mn and Si recoveries in SiMn

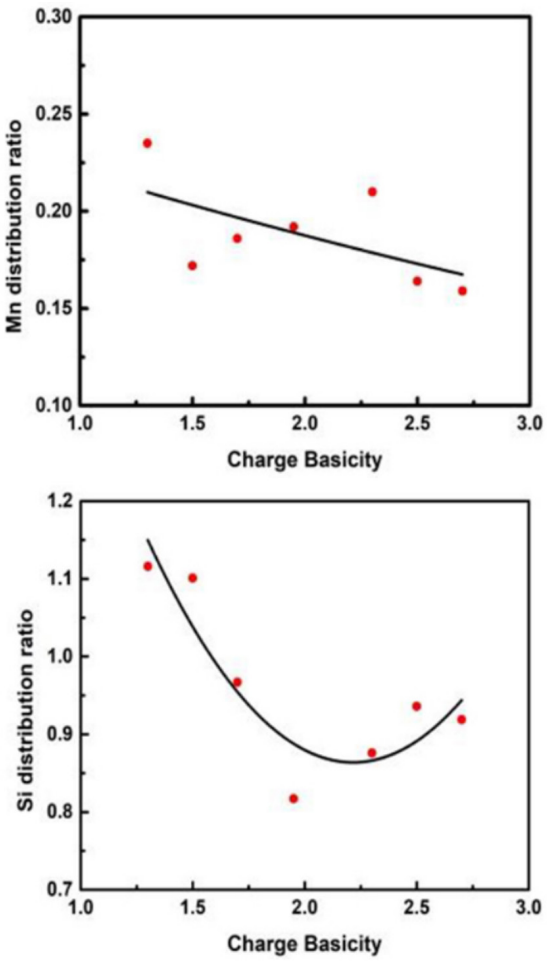

Figure 7—Effect of charge basicity on Mn and Si distribution ratio

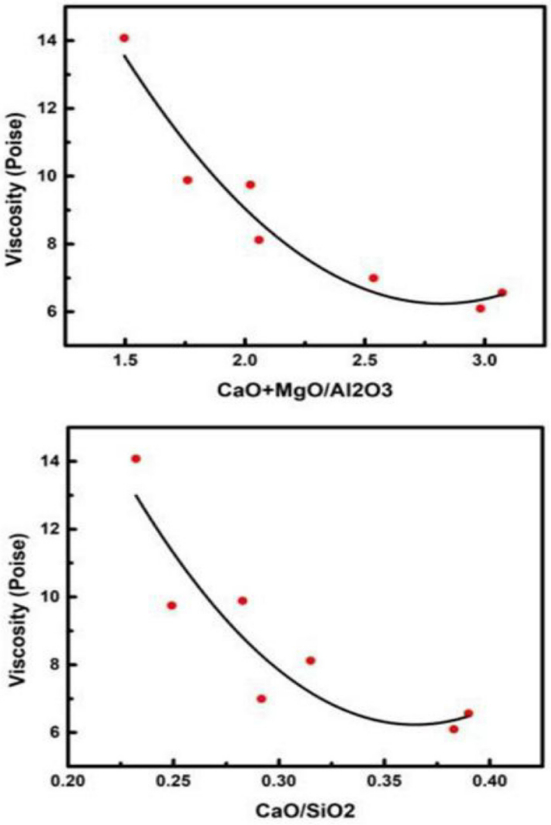

Figure 8—Effect of final slag basicity on the slag viscosity

high basicity. As indicated in Figure 4, this is due to the hindering of the sinking of metal droplets through the slag layer, which leads to entrapment of the metal droplets and thereby causes the lower metal yield and recoveries of manganese and silicon.

Effect of charge Mn/Si ratio

Four experimental heats (12, 14–16), were designed to investigate the effect of the Mn/Si ratio of the charge on manganese and silicon recoveries and metal yield. In this series, the blends were composed of manganese-rich slag (50%) and medium-grade manganese ore (25%) with a coke ratio equal to 1.35. These heats had nearly the same Mn/Fe ratio of about 5.6 and the quartzite addition was varied from 15 to 30% of the charge blend. The input raw materials of the four experimental heats were given in Table II and the chemical compositions of the product alloy and slag are shown in Table III. The effects of the Mn/Si ratio of the charge on the metallic yield and recoveries of manganese and silicon are shown in Figures 9 and 10. The metal yield and Mn recovery increased with increasing charge Mn/Si ratio up to an optimum ratio equal to 2. A further increase was accompanied by a general decrease in the metal yield and manganese recovery.

At a low Mn/Si ratio, manganese and silicon were not reduced mainly from their free oxides, but from their oxides combined as silicates as given in Equation [4]. More free SiO_2 increases the silica activity, resulting in greater silica reduction with increasing silicon recovery. On the other hand, an enhanced silica activity decreases the MnO activity by forming stable ß-manganese silicates, as indicated in Equation [10], which coat MnO particles thus minimizing the contact area between the reducing agent and MnO, which in turn decreases the manganese recovery (Coetsee,

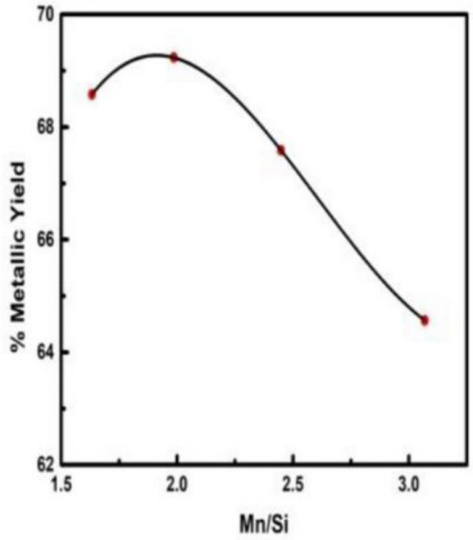

Figure 9—Effect of Mn/Si ratio on metal yield of SiMn

Zietsman, and Pistorius, 2014; Yastreboff, Ostrovski, and Ganguly, 1998; Cengizler, 1993). With increasing Mn/Si ratio, the activity of MnO increases owing to the decreasing silica content, with the result that the metal yield and recovery of manganese increase up to a Mn/Si ratio of 2. The decrease in recoveries and metal yield beyond this point can be explained by the effect of the Mn/Si ratio on the distribution of manganese and silicon between the alloy and slag phase, as shown in Figure 11. However, with the addition of silica to the slag, an $MnO.SiO_2$ type complex is formed, which limits the activity of free MnO and hence affects the reduction of MnO to Mn. Thus, with an increase in silica the silicon content increases and manganese recovery decreases. The addition of silica also increases the slag liquidus, which in turn leads to a higher bath temperature favourable for Si recovery (Olsen, Tangstad, and Lindstad, 2007; Kor, 1979; Cengizler, and Eric, 2016; Swinbourne, Rankin, and Eric, 1995).

Therefore, a Mn/Si ratio of 2 in the blend is considered the most suitable to meet the Si and Mn requirement in the silicomanganese standard (Swinbourne, Rankin and Eric, 1995). The higher silica content of the slag raises the slag viscosity and thus retards the slag/metal reactions (Kor, 1979; Ding and Olsen, 2000).

$$MnO + SiO_2 \rightarrow MnSiO_3 \quad [12]$$

Production of silicomanganese alloys on a 100 KVA pilot-scale SAF

The bench-scale tests indicated that the optimum conditions for producing a standard SiMn alloy were a coke ratio of 1.35, charge basicity 2.5, Mn/Si ratio 2, and Mn/Fe ratio 5.6. One experimental heat was carried out in triplicate in a 100 kVA pilot submerged arc furnace using these conditions. The charge composition and chemical analysis of the SiMn products are given in Table IV. The results indicate that that high-manganese slag produced by selective reduction of low-grade Egyptian manganese ore was successfully smelted on a pilot scale to produce a silicomanganese alloy containing about 65% Mn and 16–17% Si, with high manganese recovery of 68–75% and silicon recovery of 36–39%.

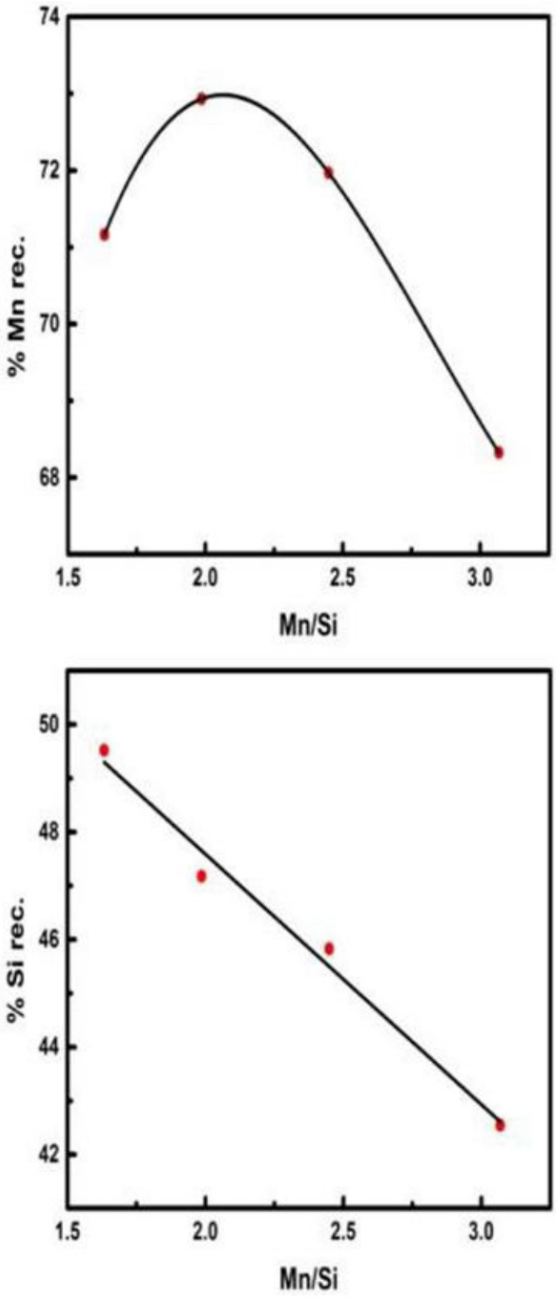

Figure 10—Effect of Mn/Si ratio on Mn and Si recoveries in SiMn

Conlusions

This work investigated the possibility of using high-manganese slag produced by selective reduction of low-grade Egyptian manganese ore and local medium-Mn ore, in a blend consisting of 50% slag, 25% medium-manganese ore, and 25% quartzite with Mn/Fe equal 5.6, to produce SiMn alloy.

Increasing the coke ratio (the ratio of added coke to the stoichiometric amount) to 1.35 leads to an increase in the metal yield and manganese and silicon recovery to the product alloy to maximum values of 66.16% , 64.13%, and 52.88%, respectively. The optimum charge basicity, expressed by $(CaO + MgO / Al_2O_3)$, that gives the higher metal yield and manganese recovery is 2.5.

The optimum Mn/Si charge ratio of 2.0 results in a metal yield (69.23%) and manganese recovery (72.93%), and a silicon recovery of 47.18%.

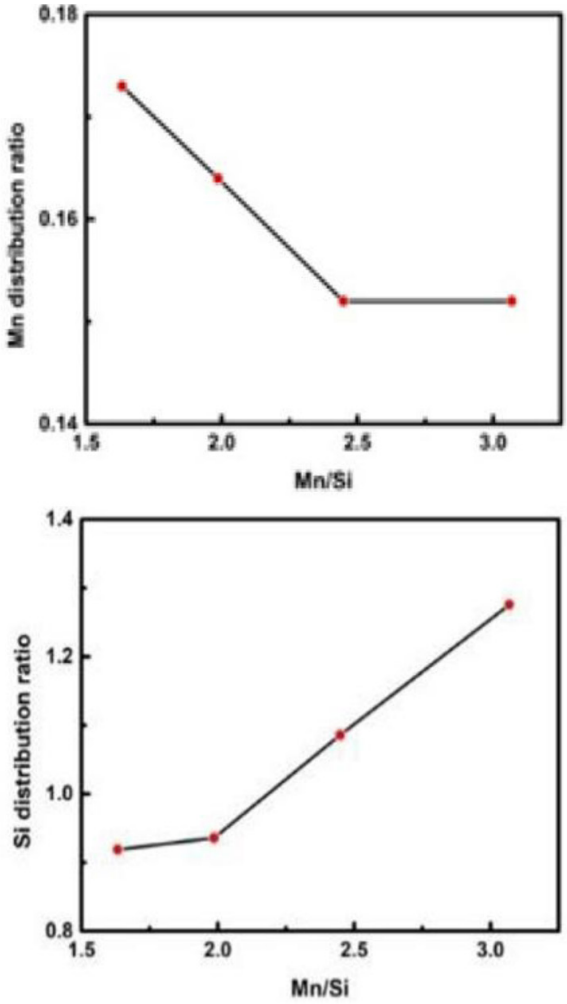

Figure 11—Effect of Mn/Si ratio on Mn and Si distribution ratios

Table IV

Experimental heats for production of SiMn in a 100 kVA pilot plant SAF

Heat no.	Charge (kg)					Metal wt.	Slag wt.	SiMn composition (wt%)					Metal	Mn recovery	Si recovery
	Mn-rich slag	Med. ore	Quartzite	Coke	Dolomite	(kg)	(kg)	C	Mn	Si	Fe	P	yield	(%)	(%)
1	22.5	15	12.5	12.5	3.27	17.5	0	2.1	64.66	16.3	Bal.	0.084	65.76	72.82	36.38
2	22.5	15	12.5	12.5	3.27	16	0	0.8	66.37	15.7	Bal.	0.046	60.13	68.34	32.04
3	22.5	15	12.5	12.5	3.27	18	1	1.1	64.8	16.93	Bal.	0.091	67.64	75.07	38.87

Based on the results of the bench-scale tests, pilot-scale tests in a 100 kVA submerged arc furnace were carried out successfully, producing a standard silicomanganese (Si16Mn63 and Si17Mn65) with high yield and recoveries.

Acknowledgements

This work was carried out a part of an applied project in a technological alliance for extending and maximizing the local beneficiation of mineral resources in Sinai, financed by the Academy of Science and Technology, Egypt. The authors would like to acknowledge the Academy of Science and Technology for financial support and the use of their facilities. Special thanks and gratitude are due to the management and colleagues in Sinai Manganese Company for the supply of raw materials, data, information, and fruitful discussions.

References

Ahmed, A., Ghali, S., El-Fawakhry, M.K., El-Faramawy, H., and Eissa, M. 2014. Silicomanganese production utilizing local manganese ores and manganese-rich slag. *Ironmaking & Steelmaking*, vol. 41, no. 4. pp. 310-320.

Akil, C. and Geveci, A. 2008. Optimization of conditions to produce manganese and iron carbides from Denizli-Tavas manganese ore by solid state reduction. *Turkish Journal of Engineering and. Environmental Science*, vol. 32, no. 3. pp. 125-131.

Alex, T.C., Godiwalla, K.M., Kumar, S., and Jana, R.K. 2007. Extraction of silicomanganese from marine and low grade mineral resources. *Proceedings of INFACON XI*, New Delhi, India, 18–21 February 2007. Indian Ferro-Alloy Producers Association. pp. 206–214. https://www.pyrometallurgy.co.za/InfaconXI/206-Alex.pdf

Anacleto, N., Ostrovski, O., and Ganguly, S. 2006. Carbon solubility and phase composition of silicomanganese. *Steel Research International*, vol. 77, no. 4. pp. 227-233.

Barin, I. 1989. Thermochemical Data of Pure Substances. VCH Verlagsgesellschaft GmbH, Weinheim. Part 2.

Bureau of Indian Standards. IS 1470: 2013. Silicomanganese –Specification,

Cengizler, H. 1993. The thermodynamic activity of MnO in manganese slags and slag-metal equilibria. PhD thesis, University of the Witwatersrand.

Cengizler, H. 2003. The manganese distribution between the metal and slag at 1500°C in ferromanganese and silicomanganese production. *Ore Dressing/Cevher Hazirlama*, vol. 9. pp. 1-5.

Cengizler, H. and Eric, R.H. 2016. Silicon and manganese partition between slag and metal phases and their activities pertinent to ferromanganese and silicomanganese production. *Advances in Molten Slags, Fluxes, and Salts: Proceedings of the 10th International Conference on Molten Slags, Fluxes and Salts 2016*. Springer, Cham. pp. 1309-1317.

Cengizler, H., Eric, R.H., and Reuter, M.A. 1997. Modeling of the activities and activity coefficients of Mn in ferromanganese slags. *Proceedings of the 5th International Conference on Molten Slags, Fluxes and Salts*, Sydney, Australia. Iron and Steel Society of AIME. pp. 75-90.

Coetsee, T., Zietsman, J., and Pistorius, C. 2014. Predicted effect of ore composition on slag formation in manganese ore reduction. *Mineral Processing and Extractive Metallurgy*, vol. 123, no. 3. pp. 141-147.

Davidsen, J.E. 2011. Formation of silicon carbide in the silicomanganese process. Master's thesis, Institute for Material Technology, NTNU, Trondheim, Norway.

Ding, W. and Olsen, S.E. 2000. Manganese and silicon distribution between slag and metal in silicomanganese production. *ISIJ International*, vol. 40, no. 9. pp. 850-856.

Eissa, M., Fathy, A., Ahmed, A., El-Mohammady, A., and El-Fawakhry, K. 2004. Factors affecting siliconmanganese production using manganese rich slag in the charge. *INFACON X. Proceedings of the Tenth International Ferroalloys Conference*, Cape Town, South Africa, 1-4 February 2004. pp. 245–253. https://www.pyrometallurgy.co.za/InfaconX/037.pdf

El-Faramawy, H., Mattar, T., Fathy, A., Eissa, M., and Ahmed, A. 2004. Silicon manganese production from manganese rich slag. *Ironmaking and Steelmaking*, vol. 31, no 1. pp. 31–36.

Emlin, B.I., Pogrebnyak, A.I., Vodin, I.I., Matyashenko, N.K., Belan, V.D., Sarankin, V.A., and Shchedrovitskii, V.Y. 1986. Silicomanganese smelting. *Otkrytiya Izobret*, vol. 30. pp. 86–88.

Jana, R.K. and Randhawa, N.S. 2009. Production of silicomanganese alloy from low manganese-containing leached sea nodules residue. *Proceedings of the Eighth ISOPE Ocean Mining Symposium*, Chennai, India 20–24 September 2009. International Society of Offshore and Polar Engineers. https://core.ac.uk/download/pdf/297715005.pdf

Kor, G.J.W. 1979. Equilibria between liquid Mn-Si alloys and MnO-SiO_2-CaO-MgO slags. *Metallurgical Transactions B*, vol. 10, no. 3. pp. 367-374.

Kubaschewsky O., Evans E.U., and Alcock C.B. 1979. Metallurgical Thermochemistry. 5th edn. Pergamon Press, Oxford.

Lagendijk, H., Xakalashe, B., Ligege, T., Ntikang, P., and Bisaka, K. 2010. Comparing manganese ferroalloys smelting in pilot-scale AC and DC submerged arc furnaces, *Proceedings of the Twelfth International Ferroalloys Congress*, Helsinki, Finland, 6–9 June 2010. https://www.pyrometallurgy.co.za/InfaconXII/497-Lagendijk.pdfs

Muller, J., Zietsman, J.H., and Pistorius, P.C. 2015. Modeling of manganese ferroalloy slag properties and flow during tapping. *Metallurgical and Materials Transactions B*, vol. 46, no. 6. pp. 2639-2651.

Nikolaev, V.I. 1974. Selection of optimum slag basicity in ferromanganese production. *Steel USSR*, vol. 4, no. 4. pp. 299-302.

Nokhrina, O.I. and Rozhikhina, I.D. 1998. Production of manganese alloys. *Izvestiya Vysshikh Uchebnykh Zavedenii, Chernaya Metallurgiya*, vol. 12.

Olsen, H. 2016. A theoretical study on the reaction rates in the SiMn production process, Master's thesis, Department of Materials Science and Engineering, Norwegian University of Science & Technologys.

Olsen, S.E. and Tangstad, M. 2004. Silicomanganese production – Process understanding. *INFACON X. Proceedings of the Tenth International Ferroalloys Conference*, Cape Town, South Africa, 1-4 February 2004. pp. 231–238. https://www.pyrometallurgy.co.za/InfaconX/012.pdf

Olsen, S.E. Tangstad, M. and Lindstad, T. 2007. Production of manganese ferroalloys. Tapir Academic Press, Norway. 249 pp.

Ray, H.S. and Pal, S. 2004. A simple method for theoretical estimation of viscosity of oxide melts using optical basicity. *Ironmaking & Steelmaking*, vol. 31, no. 2. pp. 125-130.

Riss, M. and Khodo, Y. 1967. Production of Ferroalloys. Mir Publishers, Moscow. 148 pp.

Rosypalová, S., Těháčková, L., Dobrovská, J., Dudek, R., Dobrovský, L., Žaludová, M., and Smetana, B. 2014. Verification of mathematical models for calculation of viscosity of molten oxide systems. *Metalurgija*, vol. 53, no. 3. pp. 379-382.

Steenkamp, J.D. 2020. FactSage-based design calculations for the production of high-carbon ferromanganese on pilot-scale. *Proceedings of the 11th International Symposium on High-Temperature Metallurgical Processing*. Springer, Cham. pp. 757-771.

Steenkamp, J.D. and Basson, J. 2013. The manganese ferroalloys industry in southern Africa. *Journal of the Southern African Institute of Mining and Metallurgy*, vol. 113, no. 8. pp. 667-676.

Steenkamp, J.D., Chetty, D., Singh, A., Hockaday, S.A.C., and Denton, G.M. 2020. From ore body to high temperature processing of complex ores: Manganese – A South African perspective. *JOM*, vol. 72, no. 10. pp. 3422-3435.

Swinbourne, D.R, Rankin, W.J., and Eric, R.H. 1995. The effect of alumina in slag on manganese and silicon distribution in silicomanganese smelting. *Metallurgical and Matererials Transactions B*, vol. 26B. pp. 59-65.

Tang, K. and Olsen, S.E. 2004. Thermodynamics of the MnO-containing slags and equilibrium relations associated with Mn ferroalloy productions. *Proceedings of the International Conference on Molten Slags Fluxes and Salts*, South African Institute of Mining and Metallurgy, Johannesburg. pp.19-23. https://www.pyrometallurgy.co.za/MoltenSlags2004/019-Tang.pdf

Tang, K. and Olsen, S.E. 2006. Computer simulation of equilibrium relations in manganese ferroalloy production. *Metallurgical and Materials Transactions B*, vol. 37 no. 4. pp. 599-606.

Tang, K. and Tangstad, M. 2007. Modeling viscosities of ferromanganese slags. *Proceedings of INFACON XI*, New Delhi, India, 18-21 February 2007. Indian Ferro-Alloy Producers Association. pp. 344–357. https://www.pyrometallurgy.co.za/InfaconXI/344-Tang.pdf

Tranell, G., Gaal, S., Lu, D., Tangstad, M., and Safarian, J. 2007. Reduction kinetics of manganese oxide from HC FeMn slags. *Proceedings of INFACON XI*, New Delhi, India, 18-21 February 2007. Indian Ferro-Alloy Producers Association. pp. 231-240. https://www.pyrometallurgy.co.za/InfaconXI/231-Tranell.pdf

Yastreboff, M., Ostrovski, O., and Ganguly, S. 1998. Carbothermic reduction of manganese from manganese ores and ferromanganese slag. *Proceedings of the 8th International Ferroalloys Congress*, Beijing, China, 7-10 June 1998. China Science & Technology Press. pp. 263–270. https://www.pyrometallurgy.co.za/InfaconVIII/263-Yastreboff.pdf ◆